The Journal of Physical Chemistry Letters

pubs.acs.org/JPCL Letter

Room-Temperature Phosphorescence and Low-Energy Induced Direct Triplet Excitation of Alq_3 Engineered Crystals

Hai Bi,* Chanyuan Huo, Xiaoxian Song, Zhiqiang Li, Haoning Tang, Sarah Griesse-Nascimento, Kai-Chih Huang, Ji-Xin Cheng, Lea Nienhaus,* Moungi G. Bawendi, Hao-Yu Greg Lin, Yue Wang, and Semion K Saikin*

Cite This: *J. Phys. Chem. Lett.* 2020, 11, 9364−9370 Read Online

ACCESS | Metrics & More | Article Recommendations | Supporting Information

ABSTRACT: Crystal engineering is a practical approach for tailoring material properties. This approach has been widely studied for modulating optical and electrical properties of semiconductors. However, the properties of organic molecular crystals are difficult to control following a similar engineering route. In this Letter, we demonstrate that engineered crystals of Alq_3 and $Ir(ppy)_3$ complexes, which are commonly used in organic light-emitting technologies, possess intriguing functional properties. Specifically, these structures not only process efficient low-energy induced triplet excitation directly from the ground state of Alq_3 but also can show strong emission at the Alq_3 triplet energy level at room temperatures. We associate these phenomena with local deformations of the host matrix around the guest molecules, which in turn lead to a stronger host−guest triplet−triplet coupling and spin−orbital mixing.

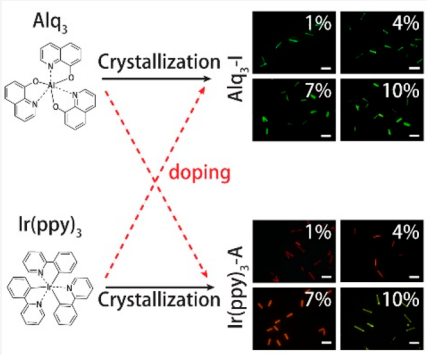

Engineered crystals—spatially ordered structures with the packing controlled by the growth process—allow for efficient modulation of optical and electrical properties of semiconductors.[1−3] However, organic crystals show low tolerance to foreign materials because of the weak intermolecular interactions.[4,5] Different types of organic molecules prefer to pack forming a new lattice structure, while barely inducing the deformation of the host lattice.[6−8] Despite the general paradigm, electronic states in organic crystals are quite localized at the molecular entities and are barely affected by proximal molecules.[6,9] Modulation of the organic crystal optical properties relies on both the inherent electronic states of the molecular entities as well as the delocalization of the molecular states.[10−14]

Electronic states of molecular entities can be of a spin-singlet or a spin-triplet character, depending on the presence of paired or unpaired electrons, respectively. Population of molecular triplet states, which is usually optically forbidden because of the requirement of an additional spin flip, can be ordinarily accomplished via intersystem crossing (ISC).[15−17] Recently, radiative decay of triplet states, which yields room-temperature phosphorescence, has become the subject of active research.[18−21] For example, including heavy atoms in the molecular structure[22,23] or inducing stronger intermolecular coupling[18,20,24] in the crystalline structure can promote the phosphorescence process. However, this mechanism still requires the excitation to higher-lying singlet states from the ground state with a subsequent ISC process to yield triplet excitons, which hinders the development of organic phosphorescence materials. Hence, direct excitation of the low-lying triplet state in the organic material, especially without involving the higher-lying singlet states, represents an intriguing strategy for modulating optical properties of organic semiconductors.[20,25,26]

We report here two types of engineered crystals that are produced by doping foreign molecules into the molecular crystalline structure. The engineered structures efficiently emit light in a broad range of the optical spectrum, which is associated with the room-temperature phosphorescence. Moreover, the emission is maintained even when the crystals are excited with incident energy below the singlet band edge of the crystals. This contrasts with pure crystals of the host or guest molecules where no photoluminescence is observed for the sub-band edge excitation. We suggest that local lattice deformations in the engineered crystals can lead to singlet−triplet intensity borrowing due to the external heavy-atom effect.[27,28] In turn, this results in the enhanced triplet optical absorption by both the host and guest complexes, as well as efficient excitation relaxation to the lowest triplet states of the host−guest system.

Received: August 7, 2020
Accepted: October 13, 2020

Downloaded via HARVARD UNIV on October 26, 2020 at 22:16:13 (UTC).
See https://pubs.acs.org/sharingguidelines for options on how to legitimately share published articles.

ACS Publications © XXXX American Chemical Society

https://dx.doi.org/10.1021/acs.jpclett.0c02416
J. Phys. Chem. Lett. 2020, 11, 9364−9370

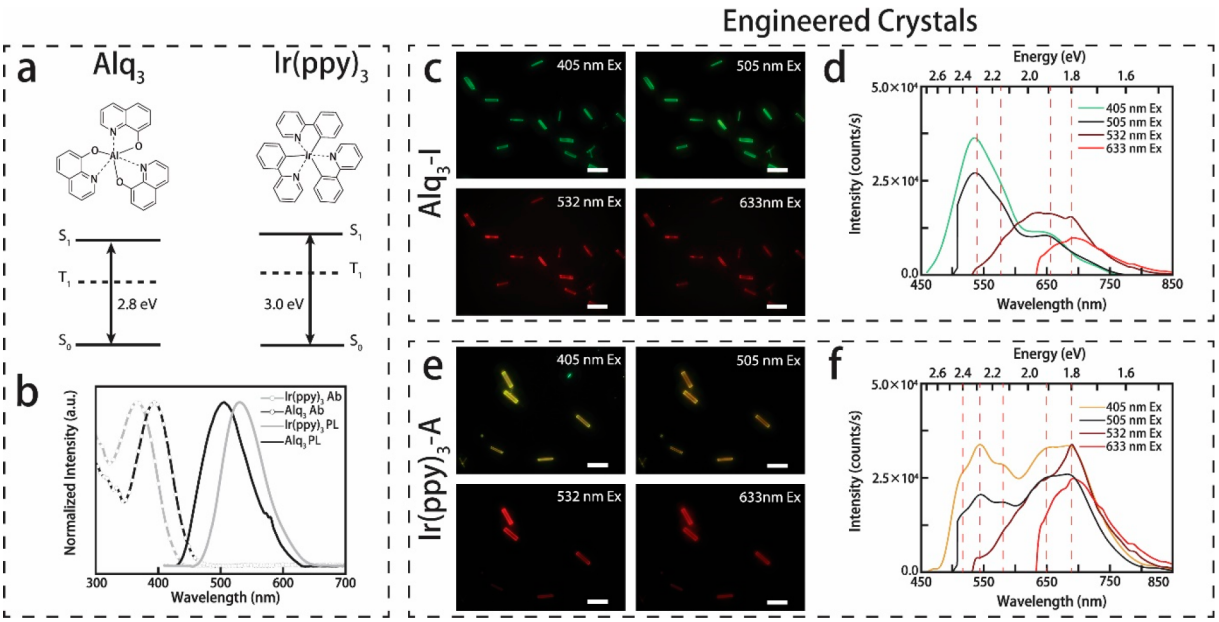

Figure 1. Photoluminescence of the Alq_3-I and $Ir(ppy)_3$-A engineered crystals. (a) Chemical structure and band gaps of Alq_3 and $Ir(ppy)_3$.[25,26] (b) Absorption and PL spectra of Alq_3 and $Ir(ppy)_3$ films. Fluorescence microscopy images of Alq_3-I (c) and $Ir(ppy)_3$-A (e) under 405, 505, 532, and 633 nm excitation at the same position. The scale bar is 10 μm. The PL spectra of Alq_3-I (d) and $Ir(ppy)_3$-A (f) engineered crystals under different excitations. The dopant concentration is 10% in both engineered crystals.

Materials based on tris(8-hydroxyquinoline) aluminum (Alq_3) and tris(2-phenyl-pyridine) iridium ($Ir(ppy)_3$) complexes (Figure 1a) are most frequently used in organic light-emitting technologies. Both structures are metal chelates, enabling molecular spatial reorganization for packing. Their performance in the optoelectronic properties,[29,30] polycrystalline phases,[31,32] and nanostructures[33,34] is widely studied both experimentally and theoretically.[35,36] The iridium complex, $Ir(ppy)_3$, exhibits the efficient long-lived triplet emission due to an internal heavy-metal effect.[37] In contrast, Alq_3 mainly exhibits flourescence, and its triplet state is hardly populated for radiative emission. Even if doped with $Ir(ppy)_3$ in the amorphous film, phosphorescence of Alq_3 can hardly be obtained at room temperatures.[33,38]

In this study, these two complexes are used for the design of engineered crystals. The energy diagrams in Figure 1a show the band gaps of the two molecules.[31,36,39] The absorption and photoluminescence (PL) spectra of these two molecules in the film are shown in Figure 1b. A significant difference in the molecular size of the complexes can induce lattice disorder in the crystalline superstructure. The modified double-film annealing method[34] is employed for the fabrication of engineered crystals at 573 K. This method allows for a fast high-temperature crystallization of the molecular material, which in turn facilitates the crystallization with the dopant. The doping percentage of the guest molecule inside the engineered crystal is controlled by the initial weight ratio of the amorphous film (see Supporting Information SI.1 for details).

Figure 1c−f shows two types of engineered crystals with a dopant concentration of up to 10% by using Alq_3 and $Ir(ppy)_3$ as the host (guest) or the guest (host) material, respectively. The crystals with the highest doping percentage equal to 10% are characterized below. Specifically, the crystals with Alq_3 as the host and $Ir(ppy)_3$ as the dopant are named as Alq_3-I (Figure 1c,d), and the crystals with $Ir(ppy)_3$ as the host and Alq_3 as the dopant are named as $Ir(ppy)_3$-A (Figure 1e,f). Excitations with the energy of 3.06 eV (405 nm), 2.46 eV (505 nm), 2.33 eV (532 nm), and 1.96 eV (632.8 nm) are employed separately for characterizing the microcrystals at the same position. Under 405 nm excitation, the Alq_3-I exhibits green PL (Figure 1c) and the $Ir(ppy)_3$-A shows yellow-white PL (Figure 1e). The PL profile of the engineered crystals remains nearly the same under 505 nm excitation. Then, the PL of the engineered crystals turns to red under 532 and 632.8 nm excitations (*cf.* Figure 1c,e).

The PL spectra corresponding to the 405, 505, 532, and 632.8 nm excitation energies are shown in Figure 1d,f (see Supporting Information SI,2 for spectra at other excitation wavelengths). Under 405 nm excitation, the spectra for both engineered crystals show double peak profiles with the maxima peak positions at 535 nm (P_1) and 670 nm (P_2). The relative intensities of these two peaks are different for the two engineered crystals, which results in the green and yellow-white emission. For peak P_1, its feature in the $Ir(ppy)_3$-A sample exhibits an additional blue-shifted shoulder at 515 nm with the main peak at 535 nm. The feature P_2 in both samples has a double-peak structure observed in the triplet emission from Alq_3 complexes.[33] Under sub-bandgap excitations, the PL spectra of the engineered crystals are as follows: 505 nm excitation can produce a PL spectrum with P_1 and P_2 simultaneously; 532 or 632.8 nm excitation results in a PL spectrum with only the P_2 part, corresponding to the red emission of the engineered crystals.

The emission lifetimes of the engineered crystals are characterized using two different excitations, 405 and 532 nm, and collecting photons with an energy below the exitation wavelength (see Figure 2). Under 405 nm (3.06 eV) excitation, the singlet state of both Alq_3 and $Ir(ppy)_3$ molecules can be sufficiently populated (see Supporting Information SI.3 for details). Both of the engineered crystals show a long-lived tail corresponding to triplet emission. The respective delayed emission lifetime of Alq_3-I is 3.01 ± 0.32 μs and of $Ir(ppy)_3$-A

https://dx.doi.org/10.1021/acs.jpclett.0c02416
J. Phys. Chem. Lett. 2020, 11, 9364−9370

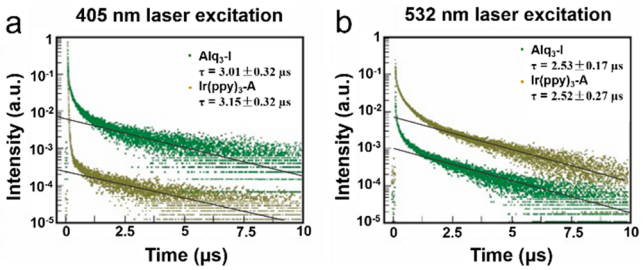

Figure 2. Time-resolved photoluminescence of Alq_3-I and $Ir(ppy)_3$-A. (a) Under 405 nm laser excitation, the late component of the curves is characterized and fitted by a mono exponential function with τ = 3.01 ± 0.32 μs for Alq_3-I and τ = 3.15 ± 0.28 μs for $Ir(ppy)_3$-A. (b) Under 532 nm laser excitation, the curves are fitted by a mono exponential function with τ = 2.53 ± 0.17 μs for Alq_3-I and τ = 2.52 ± 0.27 μs for $Ir(ppy)_3$-A. The fit curves are shown in gray.

is 3.15 ± 0.15 μs (Figure 2a). It can be inferred from the radiation lifetime test results that the inclusion of the iridium atom in the crystalline structure induces the triplet emission of the engineered crystal.

Laser excitation at 532 nm (2.33 eV), which is below the singlet bands of Alq_3 and $Ir(ppy)_3$, is employed for characterizing dynamics of subband excitations. The emission lifetime of Alq_3-I and $Ir(ppy)_3$-A are 2.53 ± 0.17 μs and 2.52 ± 0.27 μs, respectively (Figure 2b). By correlating the energy diagram with the PL spectra (*cf.* Figure 1a,d), P_2 corresponds to the triplet emission of Alq_3.[35,39] Therefore, the difference in the observed emission lifetimes with different excitations can be associated with the different decay pathway involved in the processes.

Under 405 nm excitation, the triplet emission of $Ir(ppy)_3$ and Alq_3 can be obtained simultaneously with the delayed PL from Alq_3.[39] Under 532 nm sub-bandgap excitation, mostly the triplet emission of Alq_3 contributes to the PL lifetime at the microsecond time scales. It is important to emphasize that both engineered crystals show PL from the Alq_3 triplet states, even when the energy of the excitation is below the lowest triplet states of $Ir(ppy)_3$. In the engineered crystals, the spin−orbital coupling of Alq_3 can be enhanced by the proximity of $Ir(ppy)_3$ complexes because of the external heavy-atom effect discussed in the literature previously.[27,40,41] This interaction would mix the triplet states of Alq_3 complexes with the higher-lying states of $Ir(ppy)_3$, which in turn allow both the direct absorption to triplet states as well as the efficient intersystem crossing.

The long-time exciton dynamics in low-lying Alq_3 triplet states in both engineered crystals is also characterized by measuring PL in the detection window between 630 and 800 nm with the excitation wavelength 405 nm. In this case, the contribution from the $Ir(ppy)_3$ phosphorescence, higher-lying Alq_3 triplet states, as well as time-delayed fluorescence from Alq_3 singlets are minimized. As compared to results shown in Figure 2, the longest lifetime that we observe is on the millisecond time scale for both Alq_3-I and $Ir(ppy)_3$-A structures (see Supporting Information SI.2 for details). Similar values of triplet lifetimes were obtained previously for crystalline Alq_3.[39] Additionally, Alq_3 triplet PL was measured as a function of temperature. While the triplet lifetime in $Ir(ppy)_3$-A shows thermally activated properties, where the long-lived exciton states become more emissive at higher temperatures, the triplet emission in Alq_3-I is less sensitive to temperature changes.

Crystalline structures of the doped materials with 10% of doping concentration are characterized by the X-ray diffraction (XRD). As shown in Figure 3a, the obtained Alq_3-I and

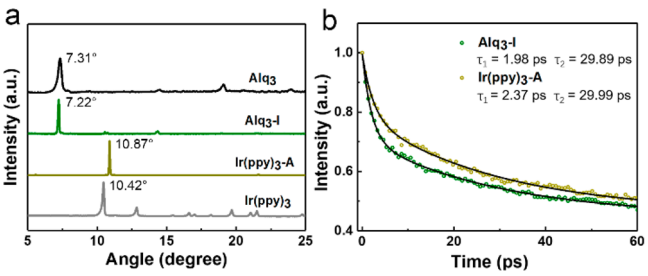

Figure 3. (a) X-ray powder diffraction spectra of the engineered crystals Alq_3-I and $Ir(ppy)_3$-A as compared to the spectra of pure Alq_3 and $Ir(ppy)_3$ crystals. Both engineered crystals show the periodicity of the host materials. (b) Characterization of the Alq_3 triplet excitation process with pump−probe measurement. The pump energy is 2.38 eV (520 nm), and the probe energy is 1.59 eV (780 nm). The black solid lines indicate the best-fits for both crystals. The curves are fit by a double-exponential function with τ_1 = 1.98 ps and τ_2 = 29.89 ps for Alq_3-I and τ_1 = 2.37 ps and τ_2 = 29.99 ps for $Ir(ppy)_3$-A.

$Ir(ppy)_3$-A structures are in a crystalline form, with fewer diffraction peaks as compared to pure crystals. By comparing these XRD profiles with those of the Alq_3 and $Ir(ppy)_3$ crystalline microwires, the prepared Alq_3-I have a clear (010) diffraction peak, which is the same as the Alq_3 crystalline structure, but with −0.09° of shift. The prepared $Ir(ppy)_3$-A shows a (220) diffraction peak which is the same as the $Ir(ppy)_3$ crystalline structure, but with 0.45° of shift. We conclude that the engineered crystals keep the crystalline structures similar to the corresponding host materials. The dopant molecules induce small shifts of the diffraction peaks, corresponding to the reduction or expansion of the crystalline lattices, which is the evidence of lattice deformation.

To compare with our engineered crystals, a homogeneous lattice deformation of pure $Ir(ppy)_3$ and Alq_3 crystals can be induced by high hydrostatic pressure.[42,43] It was shown that such a deformation further affects photoluminescence properties of the materials. These changes in photoluminescence have been explained in terms of the enhancement of molecular interactions as intermolecular distances decrease. Specifically, pure $Ir(ppy)_3$ crystals with a compressed lattice have been characterized by the occurrence of a shoulder at 507 nm at the high-energy side of the main maximum at 545 nm emission peak profile. The computational results suggest that the short-wavelength shoulder peak can correspond to the 0−0 transition, but this vibronic structure of the triplet emission spectra is rarely observed at ambient conditions.[44] The $Ir(ppy)_3$-A, where the $Ir(ppy)_3$ lattice disorder is induced by the Alq_3 dopant, shows P_1 with the shoulder peak profile which is similar to the PL spectrum of the $Ir(ppy)_3$ crystal under high pressure, verifying that P_1 is the triplet emission $Ir(ppy)_3$. In contrast, we have not observed a shoulder peak for the Alq_3-I crystal.[21] The pure Alq_3 crystal with lattice distortion under high pressure shows a significant shift to longer wavelength due to the higher proportion of triplet emission. This agrees well with the triplet emission of Alq_3 (P_2) in both engineered crystals. We hypothesize that the PL behavior of engineered crystals can be associated with the enhancement of molecular interactions as the crystal lattice is distorted by the doping molecules.

https://dx.doi.org/10.1021/acs.jpclett.0c02416
J. Phys. Chem. Lett. 2020, 11, 9364−9370

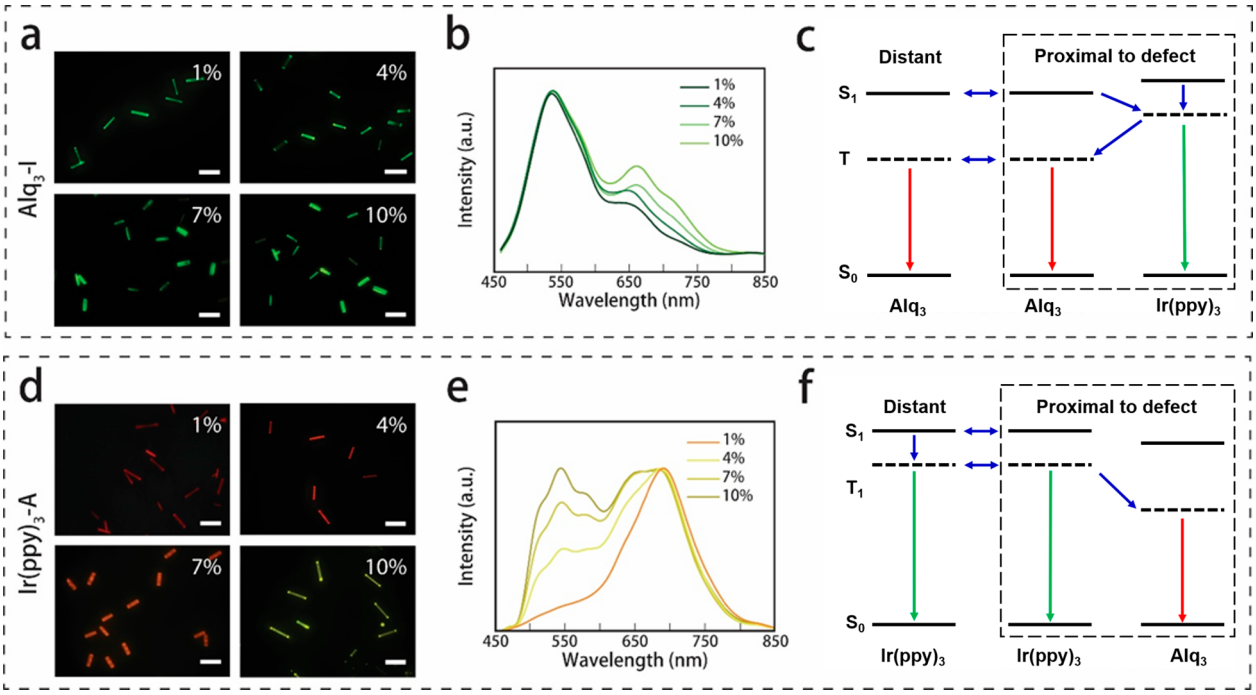

Figure 4. Alq_3-I and $Ir(ppy)_3$-A engineered crystals with different doping concentrations. (a and d) PL images of the engineered crystals with different doping concentrations under 405 nm laser excitation. The scale bar is 10 μm. (b and e) the corresponding PL spectra. (c and f) Proposed mechanisms of energy transfer. Colored (green and red) arrows correspond to different radiative relaxation processes in $Ir(ppy)_3$ and Alq_3. Blue arrows are for nonradiative inter- and intramolecular transitions. For each crystal, both distant sites and proximal to the defect molecules of the host crystal are shown.

The low-energy level structure of engineered crystals is further characterized using a transient absorption technique by exciting the samples below the P_1 peak, which are pumped at 520 nm and probed at 780 nm. Under the sub-bandgap excitation, the decay profiles for both the engineered crystals exhibit the dual decay component. The best-fit curves for the decay of two engineered crystals are shown in Figure 3b. For Alq_3-I, the decay dynamics are well fit by a double exponential τ_1 = 1.98 ps and τ_2 = 29.89 ps. For $Ir(ppy)_3$-A, we obtain τ_1 = 2.37 ps and τ_2 = 29.99 ps. The transition time scale is comparable with the ultrafast dynamics of electronic excitations in $Ir(ppy)_3$[37] and the quinolinolate complexes.[45] It can be associated with the excitation transfer between states of the same symmetry. In contrast, the pure Alq_3 or $Ir(ppy)_3$ does not exhibit any photon absorption under sub-band edge excitation (see Supporting Information SI,4 for detail). For the engineered crystals, such transitions are permitted without the excitation of their S_1. The absorption of a photon of 2.38 eV leads to the excitation of intermediate triplet states which subsequently relax to the lowest triplet state T_1. As suggested earlier, the host−guest coupling in the engineered crystals permits the intersystem crossing which is forbidden for the molecular entity or the pure crystals.

The intermolecular coupling is further investigated by varying the doping concentration in the engineered crystals (Figure 4). Under 405 nm excitation, the Alq_3-I crystals exhibit mainly green PL (Figure 4a), which is barely affected by the doping concentration. In contrast, the PL images of $Ir(ppy)_3$-A crystals vary from yellow-white to red with the change of the doping percentage from 10% to 1% (Figure 4d). As shown in Figure 4b,e, the intensity of the feature P_1 relative to the feature P_2 remains nearly the same for Alq_3-I crystals but decreases significantly for $Ir(ppy)_3$-A crystals when the doping concentration is reduced. As compared to the previous study,[39] the emission from Alq_3 triplet states is observed at room temperature for both types of engineered crystals and all studied concentrations of dopants. This supports our hypothesis of strong coupling between the triplet states of the host and the guest complexes, which in turn facilitates host−guest triplet exciton transfer.

The associated excitation dynamics is proposed as follows. In both types of the engineered crystals, the low-lying singlet states of either the Alq_3 or $Ir(ppy)_3$ molecular entity are optically populated, which further results in the intermolecular excitation transfer, intramolecular ISC, and the photon emission processes (Figure 4c,f). In Alq_3-I crystals, the generated electronic excitations diffuse through the singlet manifold of the host complexes using Förster interaction until they get trapped by $Ir(ppy)_3$ and subsequently converted into triplets.[46] The following step, the triplet−triplet transfer between the guest $Ir(ppy)_3$ and the host Alq_3, is mediated by the Dexter interaction.[38] In contrast, singlet electronic excitations in $Ir(ppy)_3$-A crystals are quickly converted into triplets and then diffuse between the host complexes by means of the Dexter interaction until they get trapped by the Alq_3 impurities. The described mechanisms are schematically outlined in Figure 4c,f, where we neglect the internal structure of the triplet and singlet bands for the sake of simplicity. The energies of the low-lying excited electronic states of the two molecules are calculated (see Supporting Information SI.5 for details) to a better understanding the energy landscape of the two systems. Both proposed processes allow the emission from the low-lying triplet states of Alq_3.

It is important to emphasize that the intensity of the feature P_1 in the PL spectra of the engineered crystals can correspond to singlet emission of Alq_3 and the triplet emission of $Ir(ppy)_3$.

https://dx.doi.org/10.1021/acs.jpclett.0c02416
J. Phys. Chem. Lett. 2020, 11, 9364−9370

Therefore, it can originate from both distant and proximal to the defect sites of the engineered crystals. In contrast, the feature P_2 is originated solely from the emission of Alq_3 triplet states. Because of the intrinsic asymmetry of the excitation transfer (Alq_3 triplet states are populated from the proximal $Ir(ppy)_3$), the P_2 features are spatially originated from the proximity of the defects in both Alq_3-I and $Ir(ppy)_3$-A structures. These differences can describe the strong variation of the relative intensities P_1:P_2 with the doping concentration in the $Ir(ppy)_3$-A materials. First, a higher concentration of Alq_3 directly results in a stronger fluorescence from a singlet state. Second, the dopant molecules deform crystal packing and alter the Dexter interaction between the triplet states of the host molecules. As compared to the Förster mechanism, the Dexter mechanism depends on the spatial overlap of molecular electronic clouds and is therefore more sensitive to the details of molecular packing. Therefore, the propagation of triple excitons has a stronger dependence on the structural defects. As the result, excitations are localized on $Ir(ppy)_3$ complexes, and a sufficient fraction of the P_1 feature is originated from these localized states. In crystals with a small concentration of defects, the triplet excitations propagate on longer distances through the host lattice and get trapped by triplet states of Alq_3 complexes.

Finally, Figure 5 illustrates the external heavy-atom effect that can describe optical excitations of Alq_3 triplet states in the engineered crystals Alq_3-I and $Ir(ppy)_3$-A. While the singlet-to-triplet transitions are forbidden in pure Alq_3, the presence of heavy atoms in neighboring molecules can result in mixing of singlets and triplets (see Figure 5b). This, in turn, allows the intersystem crossing the Alq_3 as well as the direct optical excitation of the low-lying triplets. The strength of this effect should correlate with the number and the proximity of heavy-atom-containing molecules to the probed Alq_3.

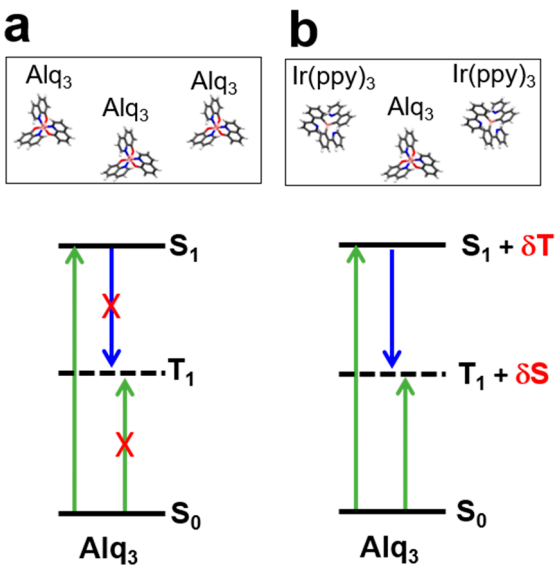

Figure 5. Schematics of the proposed external heavy-atom effect in the studied engineered crystals. The black lines represent singlet (S) and triplet (T) energy levels of Alq_3, and the vertical arrows show allowed (cross is for forbidden) transitions; green arrows are for the optical excitations, and blue arrows are for ISC. (a) The transitions between states of different spin multiplicity in Alq_3, surrounded by other Alq_3 molecules, are forbidden. (b) In contrast, in Alq_3 surrounded by $Ir(ppy)_3$, the heavy atom effect can result in the mixing of singlet and triplet states, which in turn allow the transitions between singlet and triplet states.

In conclusion, we designed and optically characterized two types of crystalline structures: Alq_3 crystals with $Ir(ppy)_3$ dopants and $Ir(ppy)_3$ crystals with Alq_3 dopants. The optical properties of the obtained organic semiconductor materials are successfully modulated by crystal engineering for the first time. Specifically, both crystals exhibit a broad range of photon absorption and emission properties. The triplet state of Alq_3 can be efficiently populated via crystal engineering. Efficient room-temperature phosphorescence of Alq_3 is observed in the engineered crystals. As compared to nondoped Alq_3 and $Ir(ppy)_3$ crystals, the engineered crystals efficiently emit light even with the excitation energy as low as 1.96 eV, which is far below the singlet bandgap of either molecule composing the crystal. The transitions between molecular energy levels within different manifolds which are otherwise forbidden by symmetry are resolved because of a stronger intermolecular coupling in the engineered crystals. We suggest that the ability to maintain the crystalline structure of the host organic materials in the engineered host−guest systems may advance multiple optoelectronic applications, including scalable crystalline solar cells, molecular photonics, and photosensitizers.

■ ASSOCIATED CONTENT

Supporting Information

The Supporting Information is available free of charge at https://pubs.acs.org/doi/10.1021/acs.jpclett.0c02416.

Additional details of the detailed experimental information, graphs and theoretical calculation methods (PDF)

■ AUTHOR INFORMATION

Corresponding Authors

Hai Bi − *Jihua Laboratory, Foshan, Guangdong, P.R. China; School of Engineering and Applied Sciences, Harvard University, Cambridge, Massachusetts 02138, United States;* orcid.org/0000-0002-2017-3668; Email: bihai@jihualab.com

Lea Nienhaus − *Department of Chemistry and Biochemistry, Florida State University, Tallahassee, Florida 32306, United States; Department of Chemistry, Massachusetts Institute of Technology, Cambridge, Massachusetts 02139, United States;* orcid.org/0000-0003-1412-412X; Email: lnienhaus@fsu.edu

Semion K Saikin − *Kebotix, Inc., Cambridge, Massachusetts 02139, United States;* orcid.org/0000-0003-1924-3961; Email: semion.saikin@kebotix.com

Authors

Chanyuan Huo − *Jihua Laboratory, Foshan, Guangdong, P.R. China*

Xiaoxian Song − *Jihua Laboratory, Foshan, Guangdong, P.R. China*

Zhiqiang Li − *Jihua Laboratory, Foshan, Guangdong, P.R. China;* orcid.org/0000-0001-7939-6543

Haoning Tang − *School of Engineering and Applied Sciences, Harvard University, Cambridge, Massachusetts 02138, United States*

Sarah Griesse-Nascimento − *School of Engineering and Applied Sciences, Harvard University, Cambridge, Massachusetts 02138, United States*

https://dx.doi.org/10.1021/acs.jpclett.0c02416
J. Phys. Chem. Lett. 2020, 11, 9364−9370

Kai-Chih Huang − *Department of Biomedical Engineering, Boston University, Boston, Massachusetts 02215, United States;* orcid.org/0000-0002-3419-825X

Ji-Xin Cheng − *Department of Biomedical Engineering, Boston University, Boston, Massachusetts 02215, United States;* orcid.org/0000-0002-5607-6683

Moungi G. Bawendi − *Department of Chemistry, Massachusetts Institute of Technology, Cambridge, Massachusetts 02139, United States;* orcid.org/0000-0003-2220-4365

Hao-Yu Greg Lin − *Center for Nanoscale Systems, Harvard University, Cambridge, Massachusetts 02138, United States*

Yue Wang − *Jihua Laboratory, Foshan, Guangdong, P.R. China;* orcid.org/0000-0001-6936-5081

Complete contact information is available at: https://pubs.acs.org/10.1021/acs.jpclett.0c02416

Notes

The authors declare no competing financial interest.

■ ACKNOWLEDGMENTS

The research described in this Letter was supported by the National Science Foundation under contract PHY1205465, the National Natural Science Foundation of China under contracts 21772064 and 21935005, and the Guangdong Basic and Applied Basic Research Foundation (No. 2019A1515110996). L.N. was supported by the Center for Excitonics, an Energy Frontier Research Center funded by the U.S. Department of Energy, Office of Basic Energy Sciences under Award Number DE-SC0001088. We warmly acknowledge financial support and discussions with Professor Eric Mazur.

■ REFERENCES

(1) Ball, J. M.; Petrozza, A. Defects in Perovskite-Halides and Their Effects in Solar Cells. *Nat. Energy* **2016**, *1*, 16149.

(2) Queisser, H. J.; Haller, E. E. Defects in Semiconductors: Some Fatal, Some Vital. *Science* **1998**, *281*, 945−950.

(3) Buonassisi, T.; Istratov, A. A.; Marcus, M. A.; Lai, B.; Cai, Z.; Heald, S. M.; Weber, E. R. Engineering Metal-Impurity Nanodefects for Low-Cost Solar Cells. *Nat. Mater.* **2005**, *4*, 676−679.

(4) Kojima, K. Crystal Growth and Defect Control in Organic Crystals. *Prog. Cryst. Growth Charact. Mater.* **1992**, *23*, 369−420.

(5) Sherwood, J. Lattice Defects in Organic Crystals. *Mol. Cryst.* **1969**, *9*, 37−57.

(6) Sun, M.-J.; Liu, Y.; Yan, Y.; Li, R.; Shi, Q.; Zhao, Y. S.; Zhong, Y.-W.; Yao, J. In Situ Visualization of Assembly and Photonic Signal Processing in a Triplet Light-Harvesting Nanosystem. *J. Am. Chem. Soc.* **2018**, *140*, 4269−4278.

(7) Sun, L.; Zhu, W.; Yang, F.; Li, B.; Ren, X.; Zhang, X.; Hu, W. Molecular Cocrystals: Design, Charge-Transfer and Optoelectronic Functionality. *Phys. Chem. Chem. Phys.* **2018**, *20*, 6009−6023.

(8) Chen, P. Z.; Weng, Y. X.; Niu, L. Y.; Chen, Y. Z.; Wu, L. Z.; Tung, C. H.; Yang, Q. Z. Light-Harvesting Systems Based on Organic Nanocrystals to Mimic Chlorosomes. *Angew. Chem., Int. Ed.* **2016**, *55*, 2759−2763.

(9) Cooper, D.; Fayer, M. Spin-Orbit Coupling in Exciton Bands of Molecular Crystals. *J. Chem. Phys.* **1978**, *68*, 229−235.

(10) Yang, Z.; Mao, Z.; Zhang, X.; Ou, D.; Mu, Y.; Zhang, Y.; Zhao, C.; Liu, S.; Chi, Z.; Xu, J.; et al. Intermolecular Electronic Coupling of Organic Units for Efficient Persistent Room-Temperature Phosphorescence. *Angew. Chem., Int. Ed.* **2016**, *55*, 2181−2185.

(11) Klimash, A.; Pander, P.; Klooster, W. T.; Coles, S. J.; Data, P.; Dias, F. B.; Skabara, P. J. Intermolecular Interactions in Molecular Crystals and Their Effect on Thermally Activated Delayed Fluorescence of Helicene-Based Emitters. *J. Mater. Chem. C* **2018**, *6*, 10557−10568.

(12) Kobayashi, Y.; Saigo, K. Periodic ab Initio Approach for the Cooperative Effect of CH/π Interaction in Crystals: Relative Energy of CH/π and Hydrogen-Bonding Interactions. *J. Am. Chem. Soc.* **2005**, *127*, 15054−15060.

(13) Mutai, T.; Satou, H.; Araki, K. Reproducible On-off Switching of Solid-State Luminescence by Controlling Molecular Packing through Heat-Mode Interconversion. *Nat. Mater.* **2005**, *4*, 685.

(14) Xie, Z.; Yu, T.; Chen, J.; Ubba, E.; Wang, L.; Mao, Z.; Su, T.; Zhang, Y.; Aldred, M. P.; Chi, Z. Weak Interactions but Potent Effect: Tunable Mechanoluminescence by Adjusting Intermolecular C-H···π Interactions. *Chem. Sci.* **2018**, *9*, 5787−5794.

(15) Leitl, M. J.; Krylova, V. A.; Djurovich, P. I.; Thompson, M. E.; Yersin, H. Phosphorescence Versus Thermally Activated Delayed Fluorescence. Controlling Singlet-Triplet Splitting in Brightly Emitting and Sublimable Cu (I) Compounds. *J. Am. Chem. Soc.* **2014**, *136*, 16032−16038.

(16) Marian, C. M. Spin-Orbit Coupling and Intersystem Crossing in Molecules. *Wiley Interdisciplinary Reviews: Computational Molecular Science* **2012**, *2*, 187−203.

(17) El-Sayed, M. Spin—Orbit Coupling and the Radiationless Processes in Nitrogen Heterocyclics. *J. Chem. Phys.* **1963**, *38*, 2834−2838.

(18) Bolton, O.; Lee, K.; Kim, H.-J.; Lin, K. Y.; Kim, J. Activating Efficient Phosphorescence from Purely Organic Materials by Crystal Design. *Nat. Chem.* **2011**, *3*, 205−210.

(19) Xiong, Y.; Zhao, Z.; Zhao, W.; Ma, H.; Peng, Q.; He, Z.; Zhang, X.; Chen, Y.; He, X.; Lam, J. W.; et al. Designing Efficient and Ultralong Pure Organic Room-Temperature Phosphorescent Materials by Structural Isomerism. *Angew. Chem., Int. Ed.* **2018**, *57*, 7997−8001.

(20) Yuan, J.; Chen, R.; Tang, X.; Tao, Y.; Xu, S.; Jin, L.; Chen, C.; Zhou, X.; Zheng, C.; Huang, W. Direct Population of Triplet Excited States through Singlet-Triplet Transition for Visible-Light Excitable Organic Afterglow. *Chem. Sci.* **2019**, *10*, 5031−5038.

(21) Tokito, S.; Tanaka, I. Phosphorescent Organic Light-Emitting Devices: Triplet Energy Management. *Electrochemistry* **2008**, *76*, 24−31.

(22) Shi, H.; An, Z.; Li, P.-Z.; Yin, J.; Xing, G.; He, T.; Chen, H.; Wang, J.; Sun, H.; Huang, W.; et al. Enhancing Organic Phosphorescence by Manipulating Heavy-Atom Interaction. *Cryst. Growth Des.* **2016**, *16*, 808−813.

(23) Koziar, J. C.; Cowan, D. O. Photochemical Heavy-Atom Effects. *Acc. Chem. Res.* **1978**, *11*, 334−341.

(24) An, Z.; Zheng, C.; Tao, Y.; Chen, R.; Shi, H.; Chen, T.; Wang, Z.; Li, H.; Deng, R.; Liu, X.; et al. Stabilizing Triplet Excited States for Ultralong Organic Phosphorescence. *Nat. Mater.* **2015**, *14*, 685−690.

(25) Yang, J.; Zhen, X.; Wang, B.; Gao, X.; Ren, Z.; Wang, J.; Xie, Y.; Li, J.; Peng, Q.; Pu, K.; et al. The Influence of the Molecular Packing on the Room Temperature Phosphorescence of Purely Organic Luminogens. *Nat. Commun.* **2018**, *9*, 840.

(26) Basu, G.; Kubasik, M.; Anglos, D.; Kuki, A. Spin-Forbidden Excitation Transfer and Heavy-Atom Induced Intersystem Crossing in Linear and Cyclic Peptides. *J. Phys. Chem.* **1993**, *97*, 3956−3967.

(27) Kasha, M. Collisional Perturbation of Spin-Orbital Coupling and the Mechanism of Fluorescence Quenching. A Visual Demonstration of the Perturbation. *J. Chem. Phys.* **1952**, *20*, 71−74.

(28) Marchetti, A. P.; Kearns, D. R. Investigation of Singlet-Triplet Transitions by the Phosphorescence Excitation Method. IV. The Singlet-Triplet Absorption Spectra of Aromatic Hydrocarbons. *J. Am. Chem. Soc.* **1967**, *89*, 768−777.

(29) Baldo, M.; Thompson, M.; Forrest, S. High-Efficiency Fluorescent Organic Light-Emitting Devices Using a Phosphorescent Sensitizer. *Nature* **2000**, *403*, 750−753.

(30) Tang, C. W.; VanSlyke, S. A. Organic Electroluminescent Diodes. *Appl. Phys. Lett.* **1987**, *51*, 913−915.

(31) Brinkmann, M.; Gadret, G.; Muccini, M.; Taliani, C.; Masciocchi, N.; Sironi, A. Correlation between Molecular Packing and Optical Properties in Different Crystalline Polymorphs and

Amorphous Thin Films of mer-Tris (8-hydroxyquinoline) aluminum (III). *J. Am. Chem. Soc.* **2000**, *122*, 5147−5157.
(32) Ide, N.; Matsusue, N.; Kobayashi, T.; Naito, H. Photoluminescence Properties of Facial- and Meridional-Ir(ppy)3 Thin Films. *Thin Solid Films* **2006**, *509*, 164−167.
(33) Tsuboi, T.; Kwon, J. H.; Liu, X.; Huang, W. The Enhanced Phosphorescence from Alq3 Fluorescent Materials by Phosphor Sensitization. *J. Photochem. Photobiol., A* **2014**, *291*, 44−47.
(34) Bi, H.; Zhang, H.; Zhang, Y.; Gao, H.; Su, Z.; Wang, Y. Fac-Alq3 and Mer-Alq3 Nano/Microcrystals with Different Emission and Charge-Transporting Properties. *Adv. Mater.* **2010**, *22*, 1631−1634.
(35) Cölle, M.; Gärditz, C.; Braun, M. The Triplet State in Tris-(8-hydroxyquinoline)aluminum. *J. Appl. Phys.* **2004**, *96*, 6133−6141.
(36) Hofbeck, T.; Yersin, H. The Triplet State of Fac-Ir(ppy)3. *Inorg. Chem.* **2010**, *49*, 9290−9299.
(37) Hedley, G. J.; Ruseckas, A.; Samuel, I. D. Ultrafast Luminescence in Ir(ppy)3. *Chem. Phys. Lett.* **2008**, *450*, 292−296.
(38) Tanaka, I.; Tabata, Y.; Tokito, S. Observation of Phosphorescence from Tris (8-hydroxyquinoline)aluminum Thin Films Using Triplet Energy Transfer from Iridium Complexes. *Phys. Rev. B: Condens. Matter Mater. Phys.* **2005**, *71*, 205207.
(39) Cölle, M.; Gärditz, C. Delayed Fluorescence and Phosphorescence of Tris-(8-hydroxyquinoline)aluminum (Alq3) and Their Temperature Dependence. *J. Lumin.* **2004**, *110*, 200−206.
(40) Xue, P.; Wang, P.; Chen, P.; Yao, B.; Gong, P.; Sun, J.; Zhang, Z.; Lu, R. Bright Persistent Luminescence from Pure Organic Molecules through a Moderate Intermolecular Heavy Atom Effect. *Chem. Sci.* **2017**, *8*, 6060−6065.
(41) Sun, X.; Zhang, B.; Li, X.; Trindle, C. O.; Zhang, G. External Heavy-Atom Effect Via Orbital Interactions Revealed by Single-Crystal X-Ray Diffraction. *J. Phys. Chem. A* **2016**, *120*, 5791−5797.
(42) Breu, J.; Stössel, P.; Schrader, S.; Starukhin, A.; Finkenzeller, W. J.; Yersin, H. Crystal Structure of Fac-Ir(ppy)3 and Emission Properties under Ambient Conditions and at High Pressure. *Chem. Mater.* **2005**, *17*, 1745−1752.
(43) Hernández, I.; Gillin, W. P. Influence of High Hydrostatic Pressure on Alq3, Gaq3, and Inq3 (Q= 8-hydroxyquinoline). *J. Phys. Chem. B* **2009**, *113*, 14079−14086.
(44) Kleinschmidt, M.; van Wüllen, C.; Marian, C. M. Intersystem-Crossing and Phosphorescence Rates in Fac-IrIII(ppy) 3: A Theoretical Study Involving Multi-Reference Configuration Interaction Wavefunctions. *J. Chem. Phys.* **2015**, *142*, 094301.
(45) Quochi, F.; Saba, M.; Artizzu, F.; Mercuri, M. L.; Deplano, P.; Mura, A.; Bongiovanni, G. Ultrafast Dynamics of Intersystem Crossing and Resonance Energy Transfer in Er(III)- Quinolinolate Complexes. *J. Phys. Chem. Lett.* **2010**, *1*, 2733−2737.
(46) Saikin, S. K.; Eisfeld, A.; Valleau, S.; Aspuru-Guzik, A. Photonics Meets Excitonics: Natural and Artificial Molecular Aggregates. *Nanophotonics* **2013**, *2*, 21−38.

https://dx.doi.org/10.1021/acs.jpclett.0c02416
J. Phys. Chem. Lett. 2020, 11, 9364−9370